IOP Conf. Series: Materials Science and Engineering **730** (2020) 012010 doi:10.1088/1757-899X/730/1/012010

Synthesis and Characterization of BiOBr Microstructures Via Free Surfactant Solvothermal Route

Yuqin Mao[1], Luping Zhu[*1], Kaixiang Liu[1], Qiang Chen[1], Yongjin Zou[2], Xinying Shen[1] and Guihong Liao[3]

[1] School of Environmental and Materials Engineering, Shanghai Polytechnic University(SSPU), Shanghai 201209, China.
[2] Guangxi Key Laboratory of Information Materials, Guilin University of Electronic Technology(GUET), Guilin 541004, China.
[3]Technical Institute of Physics and Chemistry, Chinese Academy of Sciences, Beijing 100190, China.
[4]E-mail: lpzhu@sspu.edu.cn

Abstract. This work demonstrated a facile and swift surfactant-free solvothermal synthesis of BiOBr architectures at 170°C for 6h. The structure and morphology were probed through diverse microscopy apparatus. The XRD result shows the obtained samples were well-crystallized tetragonal phase of BiOBr architecture. SEM images display these microspheres were distributed with a good polydispersity, even though most of them have inconsistent diameters. UV-vis spectrum reveals the band gap energy is approximately about 2.87 eV. The PL spectrum of the obtained BiOBr tested at room atmosphere reveals the strongest emission peaks appear at 469nm, which is in the visible region. On the basis of the above results, BiOBr samples also exhibit excellent photocatalytic performance in decomposing the organic dye RhB, which degradation efficiency reaches 99.7% after 50 min under ultraviolet light irradiation.

1. Introduction

As a layer-structured semiconductor, bismuth oxybromide (BiOBr) with tetragonal matlockite structure that $[Bi_2O_2]^{2+}$ slabs interleaved by double slabs of halogen atoms[1]. Besides this, bismuth oxybromide is interesting, not only as a good catalysts for degrading rhodamine-B (RhB)[2] or methyl orange (MO)[3], but also because of their special and excellent physical-chemical properties with other potential applications in ferroelectric materials, pigments, and catalytic fields[4-6]. Generally speaking, the properties of materials mainly rely on their size, structure, and dimensions. Considerable efforts have been devoted to the fabrication of BiOBr. For example, Xiong and co-workers prepared three-dimensional flower-like BiOBr nanoarchitectures through the direct transform of metallic Bi nanospheres[7]. Cheng's group prepared BiOBr hollow microspheres via a one-step Miniemulsion-Mediated route[8]. Zhang et al reported the synthesis of 3D flower-like BiOI nanoplates by an simple EG-assisted solvothermal method[9]. Inspired by previous work, we proposed a facile and mild surfactant-free solvothermal process to fabricate BiOBr microspheres. The optical and photocatalytical preformances were examined by UV-vis spectroscopy and fluorometer.

2. Experimental

2.1. Preparation of BiOBr Microspheres

Preparation of BiOBr Microspheres

All chemicals used in this work were purchased from the Shanghai Experiment Reagent Corporation Ltd. and were utilized as received without any further purification. In a typical experiment, 1.5 mmol $Bi(NO_3)_3 \cdot 5H_2O$ was mixed in 30 mL of ethylene glycol (EG) with vigorously stirring until $Bi(NO_3)_3 \cdot 5H_2O$ was dissolved completely. Then, 8.0 mmol NaBr was introduced into the former solution with stirring at room temperature. Subsequently, a transparent precursor was obtained and placed into a Teflon-lined stainless steel autoclave (50 mL), and then sealed and heated at 170°C for 6h at the same time. Finally, when the autoclave was cooled to room temperature naturally, the resulting white precipitate was collected, then wash with deionized (DI) water and absolute ethanol three times and dried at 80°C in air.

2.2. Photocatalysis Experiments

The photocatalytic efficiency of the obtained BiOBr samples was investigated by degrading Rhodamine-B (RhB) under UV light irradiation (λ=365nm), as described in our previous works[10-11].

2.3. Materials Characterizations

The phase purity of the products were measured by X-ray diffractometer (XRD, Rigaku D/max 2500). The overview of the sample morphology was characterized by scanning electron microscope (SEM, Hitachi S-4800), in conjunction with a system of energy-dispersive spectroscopy (EDS) analysis. Diffuse reflectance UV-vis of the powders were carried out by UV-vis spectrophotommeter (Shimadzu 2550), and photoluminescence (PL) spectrums were conducted by fluorometer (Hitachi F-4500) with a Xe lamp as the excitation light source at room temperature. Moreover, the concentrations of the RhB were measured by Shimadzu 2550 spectrophotommeter at 553nm during the photodegradation process.

3. Results and Discussion

The XRD pattern of the product is shown in Figure 1(a). The narrow broadening of peaks displayed a well-crystallized BiOBr material, and can be allocated to the tetragonal phase of BiOBr structure (JCPDS card no.73-2061). Consistent with the XRD results, the EDS pattern illustrated in Figure 1 (b) reveals the product includes Bi, O, and Br elements is approximately equal to 1:1:1.

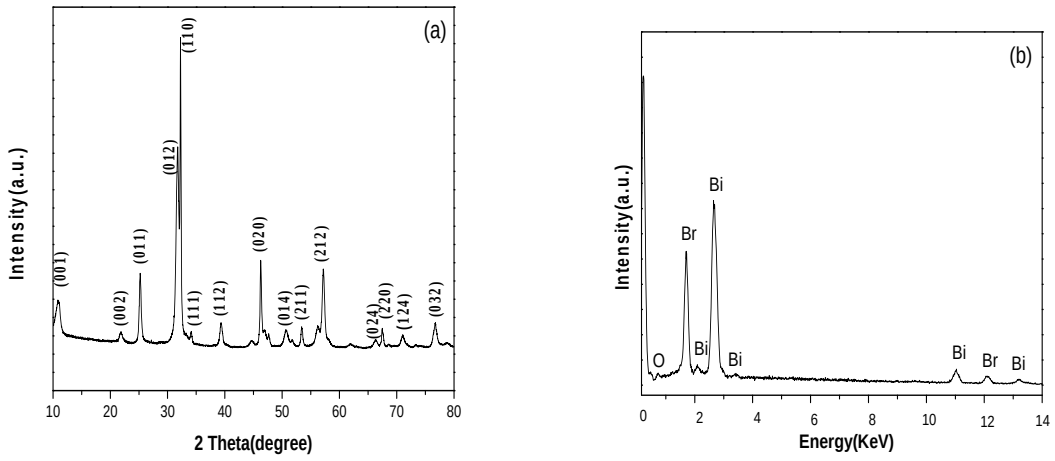

Figure. 1 Powder XRD (a) and EDS (b) patterns of BiOBr micropheres.

The morphology of the BiOBr microspheres fabricated by a surfactant-free solvothermal method are shown in Figure 2 (a-c). The SEM image with low-magnification manifests that the product composes of numerous microspheres with diameters ranging from 2 to 6 μm. An individual BiOBr microsphere is shown in Figure 2 (b)-(c) reveals the exterior surfaces of microspheres are not obviously smooth but involve many radially grown nanosheets.

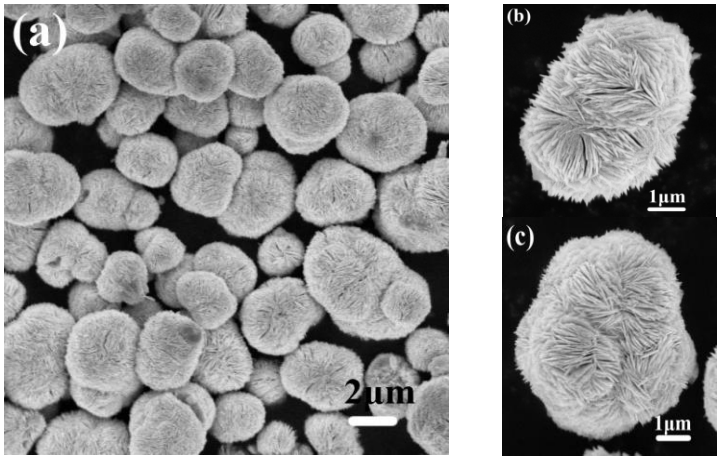

Figure. 2 SEM images in low-magnification (a), and a single BiOBr at various angle : (b) declivitous, (c) left-oblique.

Figure 3 (a) depits the UV-vis diffuse reflectance spectrum of BiOBr microspheres. Assuming BiOBr is an indirect semiconductor, the $(\alpha h\nu)^{1/2}$ versus photon energy hν curve for the BiOBr samples can be shown in the inset of Figure 3 (a). The extrapolates value (the straight line to the X-axis) of band gap energy (Eg value) at $\alpha = 0$ gives an absorption edge energy corresponding to Eg = 2.87 eV, which is in the visible light region. The Eg values were a slight different from the theoretic value (2.54 eV)[12], which could be ascribed not to the transition from the impurity to the conduction band but to the intrinsic transition between the valence band and the conduction band.

The photoluminescence property of the flower-like BiOBr excited at 270nm at room temperature is demonstrated in Figure 3 (b). It can be observed that the PL spectrums of the prepared samples are in the visible region (390 - 550 nm). Moreover, the strongest PL emission peaks appear at 469 nm. According to the literature[13-14], the PL intensity may be attributed to the morphology, particle size, and surface defects.

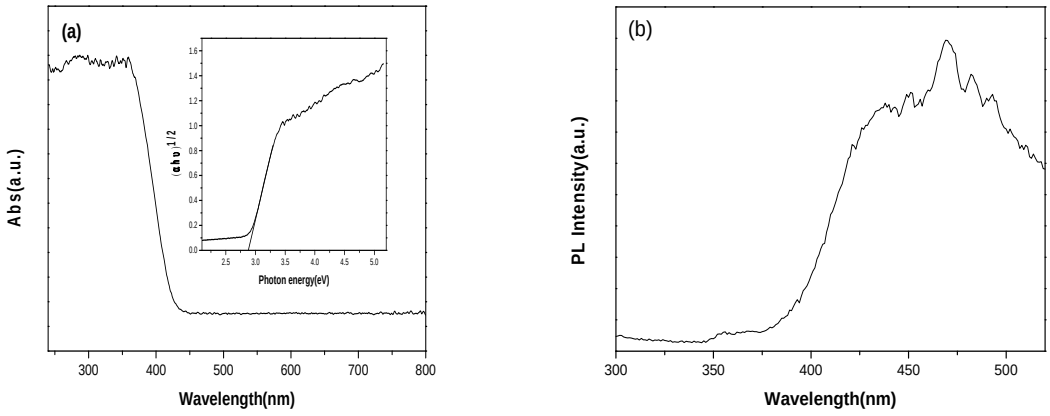

Figure. 3 UV-vis diffuse reflectance spectrum (a) and PL spectrum (b) of the flower-like BiOBr. Inset : the $(\alpha h\nu)^{1/2}$ - hν curve for the products.

The variations of RhB concentration (C/C_0) with different catalyst loading can be described in Figure 4 (b). It is note worthy that the absence of both light source and catalysts are negligible for efficient degradation. Therefore, as to photocatalytic activities, catalysts and illumination are of great importance. Generally, catalyst loading plays a critical part in the control of recombination of holes and electrons of BiOBr samples. Hence we probed with different catalyst loading ranging from 5 mg to 20 mg, while the concentration of RhB and light source remained constant. The results clearly show that the degradation efficiency reaches 89.2%, 96.1%, 99.7% for samples 5mg, 10mg, and 20mg with 50 min, respectively. Thereby, the suggested catalyst dosage is 20mg.

Figure 4 (b) demonstrates the UV-vis spectra of RhB (10mg/L) degradation on BiOBr (20mg) for time intervals of 0-50 min. The results show that the absorption peak diminishes progressively as the exposure time increases and completely vanishes after 50 min, which means that 99.7% of the RhB degradation was achieved in 50 min, which is consistent with UV and PL results.

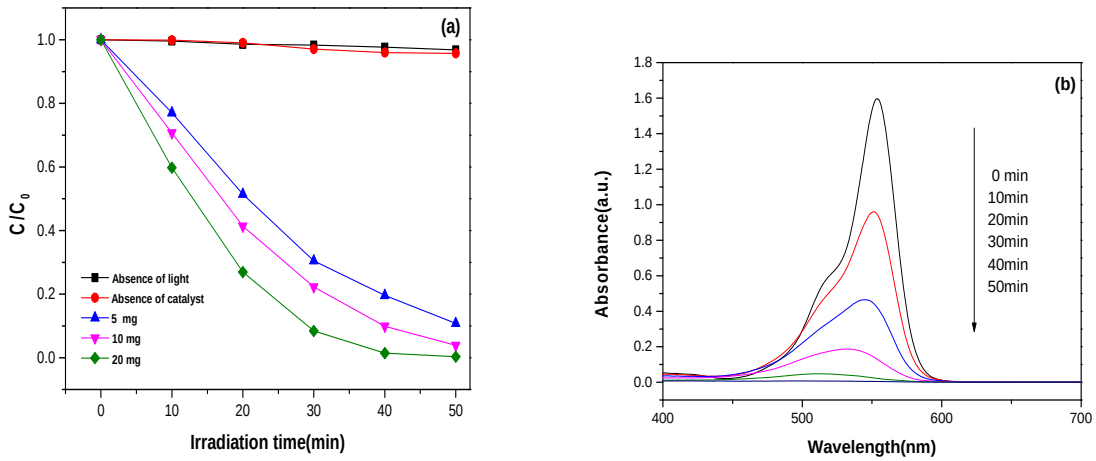

Figure. 4 (a) photocatalytic performances of different catalyst loading:5mg, 10mg, and 20mg. (b) absorption spectra of a solution of RhB in the presence of the BiOBr products (20mg) under ultraviolet light exposure.

4. Conclusions

In summary, flower-like BiOBr with high crystallinity are successfully synthesized by a simple surfactant-free solvothermal method. Flower-like BiOBr in the rang of 2- 6 μm were observed which were confirmed by SEM analysis. UV-vis demonstrates the samples prepared at 170°C show the band gap energy were about 3.07 eV. The PL spectrum indicates that the powders possess a strong and broad emission in the visible region (390-550nm), in which the strongest emission peak appears at 469nm. The suggested catalyst loading is 20mg, which the degradation efficiency reaches 99.7% in 50min. The present work suggests that these 3D BiOBr architectures may be offer new potentials in semiconductor photocatalysis, solar cells, optic and gas sensing applications.

5. Acknowledgments

This research was jointly supported from the Shanghai Municipal Natural Science Foundation (No: 18ZR1415700), the Guangxi Key Laboratory of Information Materials (GUET) (No:171011-K), the Leap Project and Postgraduate fund (SSPU) (Nos: EDG18XQD26, EGD18YJ0049), the key subject of SSPU (No. 4: Material Science and Engineering, XXKZD1601), and the Gaoyuan Discipline of Shanghai–Environmental Science and Engineering (Resource Recycling Science and Engineering).

6. References

[1] Zhang K, Liu C M and Huang F Q 2006 *Appl Catalysis B* **68** 125-9

[2] Zhang L, Cao X F and Chen X T 2011 *J Coll Interface Sci* **354** 630-6
[3] Jiang Z, Yang F and Yang G 2010 *J Photochemistry and Photobiology A* **212** 8-13
[4] Kusainova A M, Stefanovich S Y and Irvine J T 2002 *J Mater Chem* **12** 3413-8
[5] Maile F J, Pfaff G and Reynders P. 2005 *Progress in Organic Coatings* **54** 150-63
[6] Huo Y, Zhang J and Miao M 2012 *Appl Catalysis B* **111** 334-41
[7] Xiong J, Dong Q and Wang T 2014 *RSC Adv* **4** 583-6
[8] Cheng H, Baibiao Huang and Wang Z 2011 *Chemistry* **17** 8039-43
[9] Zhang B, Ji G and Gondal M A 2013 *J Nanoparticle Res* **15** 1773
[10] Mao YQ, Li YH and Zou YJ 2019 *Cera Inter* **45** 1724-9
[11] Zhu LP, Liao GH and Bing NC 2010 *CrystEngComm* **12** 3791-6
[12] Zhang J, Shi F and Lin J 2010t *Chem Mater* **39** 2937-41
[13] Zhu LP, Wang LL and Bing NC 2016 *RSC Adv* **6** 2926-34
[14] Zhu LP, Mao YQ and Chen Q 2019 *J Mater Sci* **30** 3639-46